Co-published by
Institute of Fluid-Flow Machinery
Polish Academy of Sciences
Committee on Thermodynamics and Combustion
Polish Academy of Sciences

http://www.imp.gda.pl/archives-of-thermodynamics/

ARCHIVES OF THERMODYNAMICS

Experimental research of a pumping engine in a micro-ORC system with a low-boiling medium

Tomasz Z. Kaczmarczyk[a]*

[a]Institute of Fluid-Flow Machinery, Polish Academy of Sciences, ul. Fiszera 14, Gdańsk 80-231, Poland
*Author email: tkaczmarczyk@imp.gda.pl

Received: 14.05.2024; revised: 11.10.2024; accepted: 29.10.2024

Abstract

The paper presents the results of experimental research on a pumping engine with the low-boiling medium HFE-7100. The research was conducted in a micro-ORC system with an output of about 2.5 kW_e. Among other factors, the impact of working medium temperature and pump rotational speed on the operating parameters of the gear pump and pumping engine is analyzed. The research shows that increasing the rotational speed and HFE-7100 temperature resulted in an increase in the power consumed by the pump drive and an increase in the effective power of the pump. The increase in the effective power of the pump was greater than the electrical power consumption of the pump drive, resulting in an increase in the volumetric efficiency of the pump. It has been established that, at a constant pump rotational speed of 2000 rpm, increasing the average temperature of HFE-7100 by 27 K from approximately 304 K resulted in a 4% increase in the pump's volumetric efficiency to 80%. It has been established that, for any value of pump rotational speed and working fluid temperature, there exists an optimal effective power value for the pump at which the pumping engine achieves the maximum efficiency.

Keywords: Gear pump; Pumping engine; HFE-7100; Micro-cogeneration; ORC system

Vol. 45(2024), No. 1, 125–140; doi: 10.24425/ather.2024.152002

Cite this manuscript as: Kaczmarczyk, T.Z. (2024). Experimental research of a pumping engine in a micro-ORC system with a low-boiling medium. *Archives of Thermodynamics*, 45(4), 125–140.

1. Introduction

Today, the world is seeing a continuous increase in the demand for electricity [1]. This has contributed to increased exploration and use of energy resources [2], rising energy prices [3], and the energy crisis [4]. This has caused an increase in the emission of pollutants into the natural environment [5]. As a result, many countries have tightened standards, restrictions and rigour related to the emission of pollutants into the environment [6]. Such actions have forced the search for new energy-saving technologies [7] and rational energy management [8], among other things. This involves, among other things, recovering waste energy [9,10], using renewable energy sources (RES) [11], or searching for new high-efficiency systems [12] and energy machines [13]. One possibility that meets the above requirements is the use of combined heat and power (CHP) systems [14], including organic Rankine cycle (ORC) technology [15].

It should be mentioned that ORC systems can be powered by heat sources with a wide temperature range [16]. These systems can use, among other things, waste heat [17] or RES [18], i.e. biomass [19], geothermy [20] or solar energy [21]. It should be noted that in ORC systems, in addition to expansion units (EUs),

Nomenclature

d – diameter, m
Eu – Euler number, $Eu=\Delta p/\rho v^2$
f – frequency, 1/s
g – gravitational acceleration, m/s^2
H – head, m
L – characteristic dimension, m
m – mass flow rate, kg/s
n – rotational speed, rpm
N – power, W
p – pressure, kPa
P – net pump power, W
q – volumetric flow rate, m^3/s
R – range
Re – Reynolds number, $Re=\rho vL/\mu$
t – temperature, °C
v – velocity, m/s
V – elementary capacity, m^3/rev
w – velocity, m/s
x – quality

Greek symbols

Δ – difference
η – efficiency, %
μ – dynamic viscosity, Pa s
ρ – density, kg/m^3
ω – angular velocity, rad/s
Ω – specific speed

Subscripts and Superscripts

1,2 – ordinal numbers
av – average
e – electrical
i – inner
nom – nominal
min – minimal
PE – pumping engine
r – real (measured)
t – thermal
th – theoretical
vol – volumetric
u – effective

Abbreviations and Acronyms

BWR – back work ratio
CHP – combined heat and power
EES – Engineering Equation Solver
EV – expansion valve
EU – expansion unit
GWP – global warming potential
MTG – micro turbogenerator
MR – measurement range
MV – measurement value
ORC – organic Rankine cycle
PE – pumping engine
RES – renewable energy sources
R1 – first temperature range
R2 – second temperature range
VSD – variable speed drive

flow units [22,23] and volumetric units [24], pumping engines (PEs) are essential components [25]. PEs not only determine the proper operation of the entire cogeneration system [26] but also the profitability and investment payback period [27].

One indicator determining the operating efficiency of cogeneration systems is the back work ratio (BWR), which is the ratio of the electrical power consumed by PE to the power produced by EU [28]. BWR is an important indicator considered in sensitivity analysis [29] and the optimisation process [30] of ORC systems with gas turbines [31]. Studies [32] show that BWR is directly correlated with the evaporation temperature of the working medium (R123) and has extremes at which the BWR value is minimum. The value of the BWR indicator depends on the type of working medium. For the same evaporation temperature value, the BWR value of the organic mediums used in ORC systems is higher than that obtained for water. As the critical temperature of the working medium increases, the BWR value decreases [33]. That is why in organic Rankine cycles, unlike in classical steam cycles, the BWR indicator can have a high value. That is why it can significantly affect the efficiency of the ORC system and even cause it to be negative [34]. Then the electric power consumed by PE is greater than the total electric power produced by the expansion unit(s) operating in the micro-ORC system [7].

Therefore, the efficiency of these power machines, and thus their energy intensity, should be as low as possible [35]. That is why new organic media are continually being tested in ORC systems to achieve the lowest possible BWR values [36]. However, it should be emphasised that pumps are mostly designed to operate with water as the working fluid [37]. Meanwhile, the physico-chemical properties of organic working media differ significantly from those of water [38]. Many a time such liquids have much higher density and lower viscosity in relation to water [39]. As a consequence, they can cause higher losses due to internal leaks in pump components and reduce their efficiency and effective delivery head [40]. Additionally, the working fluids used in ORC systems can have adverse effects on pump [41] and microturbine components [42,43], and they can also cause cavitation [44,45]. These phenomena can contribute to machinery malfunctions, which can eventually lead to their damage or breakdown. Therefore, to prevent and eliminate these adverse effects, analyses [46] and numerical simulations [47] are conducted, as well as experimental research [48] when these machines operate in conjunction with each other in ORC systems [49].

For example, Yang et al. [50] conducted a study on a multi-stage centrifugal pump, hydraulic diaphragm metering pump and roto-jet pump in an ORC system with R245fa refrigerant. The study was conducted with a working fluid temperature at the pump supply of approximately 30°C and a pressure range of 4 to 11 bar. They determined that the maximum efficiencies of these pumps were 58.76%, 55.26% and 30.51%, respectively. On the other hand, the maximum mechanical efficiency of the multistage centrifugal pump operating in an ORC system with R245fa fluid was approximately 62% [51]. Zeleny et al. [52] conducted a study on a PE with a gear pump operating in an ORC system with a nominal electrical power of approximately 5 kW_e. The pump was supplied with the working fluid, hexamethyldisiloxane. The study shows that, at the operating point of the ORC unit, the maximum isentropic and volumetric efficiencies were approximately 70% and 81%, respectively, and the PE efficiency was approximately 45%. D'Amico et al. [53] conducted a study on a multi-diaphragm pump in a 5 kW_e ORC system. They used R134a as the working fluid. For the nominal operating parameters of the ORC system, the working fluid temperature at the pump supply was approximately 30°C. The study showed that with a differential pressure of approximately 15 bar in the pump, the maximum PE efficiency was approximately 32%, and the maximum volumetric efficiency of the pump was around 94%.

Carraro et al. [54] studied a PE with a multi-diaphragm pump in a 4 kW_e ORC system with R134a as the working fluid. The pump, operating at a supply frequency of 50 Hz, had a rotational speed of 960 rpm and could generate a maximum pressure of approximately 25 bar. The study shows that an important parameter affecting the efficiency of PE is the pump rotational speed. They determined that as the rotational speed of the pump increases, the efficiency of PE increases. At 53% of the rated frequency of the pump drive supply and within a working fluid pressure differential range of 7 bar to 15.5 bar, the efficiency of PE was in the range of 15–24%. When the drive supply frequency was increased to 80% of the rated value, and the rotational speed of the pump was thus increased to 782 rpm, a pressure differential of 15 bar and a maximum PE efficiency of approximately 48% were achieved. On the other hand, further increases in the rotational speed of the drive resulted in a decrease in PE efficiency. Numerical analysis by Zardin et al. [55] shows that at low rotational speeds and high forcing pressures, so-called critical operating conditions arise, resulting in an approximate 15% decrease in the mechanical efficiency of the gear pump.

A study by Misiewicz [56] shows that as the load rate and rotational speed decrease, the efficiency of an electric motor operating in conjunction with a frequency converter decreases. The researchers found that an electric drive operating below 70% of the rated load could result in a reduction in the efficiency of the pump unit by approximately 57%. Similar conclusions were obtained by Yang et al. [57], who studied a piston pump in an ORC system with R123 fluid. The study shows that at low rotational speeds (approximately 8 Hz), the maximum efficiency of PE was around 30%, with the pump's maximum isentropic efficiency of approximately 73%.

However, the total efficiency of PEs used in micro-ORC systems depends not only on the pump efficiency but also on the efficiency of the pump drive and additional equipment, e.g. inverter, etc. For example, a study conducted by Landelle et al. [58] on a PE unit with a reciprocating pump in an ORC system with R134a fluid shows that, regardless of the pump's rotational speed and discharge pressure, the power consumption of the variable speed drive (VSD) is constant. The power balance presented for the PE unit shows that at a maximum pressure of 35 bar and about 33% of the rated rotational speed of the pump, the power lost by VSD was about 44%, and the effective power of the pump was about 40% of the total power of the PE unit. On the other hand, pump and motor losses were 13% and 3%, respectively. Under the rated operating conditions of the pump, the effective power of the pump accounted for approximately 52% of the total power of the PE unit, and the losses in VSD, motor and pump were 19%, 12% and 17%, respectively. The researchers found that at the rated rotational speed of the pump, as the forcing pressure decreases, the effective power of the pump decreases, and the losses in VSD, motor and pump increase.

Feng et al. [59] conducted a study on a plunger pump operating in an ORC system with a capacity of approximately 2 kW_e. The cogeneration system used an expansion unit with a scroll expander, which was powered by the R123 fluid. The study found that the isentropic efficiency of the scroll expander was in the range of 69% to 85%. The researchers determined that the efficiency of the electric generator was in the range of 60% to 73%. On the other hand, the isentropic efficiency of the plunger pump was in the range of 27% to 54%. For these operating conditions of the cogeneration system, the BWR value was in the range of 14% to 32%. The work highlights that the maximum theoretical thermal efficiency of this cycle was approximately 11%, and the maximum thermal efficiency confirmed by the study was about 5%. On the other hand, a study [60] conducted on a diaphragm metering pump in an ORC system with R123 fluid demonstrates that as the BWR indicator increases, the thermal efficiency of the cycle decreases. On the other hand, the ORC system's thermal efficiency was 0.13% and was similar to the results obtained by Gao et al. [61].

On the other hand, Komaki et al. [62] found that an alternative to commercial solutions could be a rotary jet pump (known as a Pitot pump), which could ensure not only a higher delivery head but also a higher flow at a higher efficiency. Literature data [63] show that the delivery head of a Pitot tube pump can be approximately 1.6 times higher than that of a conventional centrifugal pump operating at the same speed. Because in this design (Pitot pump), high rotational speeds of the pump are not necessary to generate high forcing pressure. In addition, the Pitot pump can also produce high pressure of the liquid at a low flow rate of the working fluid.

As part of the literature review, it is worth mentioning that research is also being conducted on so-called pumpless ORC systems. A study by Jiang et al. [64] demonstrated that the maximum electrical efficiency of a pumpless ORC system with a 1 kW_e scroll expander powered with R245fa was 2.4%. Theoretical calculations by Gkimisis et al. [65] demonstrate that pumpless micro-ORC systems can achieve a maximum thermal efficiency of approximately 5%. On the other hand, according to Richardson [66], in the case of two-stage systems with thermofluidic pumps, the theoretical efficiency of these ORC systems can be approximately 7.5%. However, it should be emphasised that these systems require advanced control and regulation systems and have a more complex structure compared to systems with PEs.

The conducted review of the thematic literature shows that, despite high pump efficiencies [67], the efficiency of the remaining components of the unit also has a fundamental impact on the total efficiency of the PE. As a result, the maximum efficiencies of PEs operating in micro-ORC systems did not exceed 48%. Moreover, the application of a different operating medium to the same type of pump gives different results obtained during experimental tests. As the review shows, the results obtained by experimental testing differed significantly from those obtained during theoretical calculations. For example, the theoretical efficiencies of the pumps and PEs were more than twice as high as the efficiencies noted during the experimental research. Hence, one can see the existing necessity to conduct experimental research on PEs operating in micro-ORC systems.

The paper presents a study conducted on a PE with a gear pump and the low-boiling fluid HFE-7100. Currently, there is a lack of experimental study on PE with such a medium in the thematic literature. It should be emphasised that HFE-7100 is environmentally friendly and possesses good thermodynamic properties as a potential working fluid for ORC systems. The HFE-7100 medium has a GWP value of 320, which is significant in terms of environmental assessment [69]. However, this medium is categorised as a solvent, which, consequently, can have an adverse effect on some construction materials of the pumps, as demonstrated in this work. That is why the experimental research results presented can also have a practical application in addition to the scientific aspects. Moreover, the research presents the effect of changing the temperature of the working fluid on the operating parameters and performance of the pump and PE, which will certainly contribute to filling the existing literature gap in this subject area. The work presents the performance characteristics of the PE and the pump based on dimensionless numbers, which will facilitate other researchers in comparing their research results and analyses. The PE characteristics presented as a function of dimensionless numbers enable researchers to compare their research results for different types of pumps effectively, spanning a wide power range. Moreover, it will be possible to compare PE research for the various working mediums used in ORC systems. The author's motivation and rationale for conducting experimental research, based on the author's experience, are presented in Section 2.

2. Motivation and rationale for conducting the experimental research

Most pumps available on the commercial market mainly have operating characteristics specified for water as the working medium. Manufacturers do not always provide the operating characteristics of pumping engines specified for the new working mediums used in ORC systems. It should be noted that there is also limited information on the durability and compatibility of pump construction elements for these new operating mediums. That is why, in the commercial market, the selection of pumping engines with the required operating parameters for the ORC system with the HFE-7100 medium was largely limited. It should be emphasised that the cost of purchasing a commercial PE is several times less than the price to be paid for individually designing and building a prototype pumping engine [49]. This means that using a commercial PE in an ORC system can be justified economically, as it can significantly reduce the total cost of the microsystem.

In ORC micro-CHP systems, pumping engines are characterised by specific operating conditions due to the required high pressure and low flow rate of the working medium in the cycle [68]. For example, for an ORC system with a 2.5 kW_e microturbine, a nominal supply pressure of approximately 1100 kPa is required at an HFE-7100 medium flow rate of approximately 0.17 kg/s [70].

The study [38] conducted on a commercial PE with a PK70-type rotodynamic pump showed that the pump's discharge pressure rise was too low in relation to the HFE-7100 medium flow rate ($\Delta p/m$). As a result, at the required nominal vapour pressure at the inlet of the expansion valve, the value of the working medium flow rate was several times higher than the nominal value. This resulted in the micro-ORC system with a 25 kW_t biomass boiler not being able to generate vapour at the required parameters, thus failing to ensure the appropriate superheating degree of HFE-7100 directed to the expansion unit. Supplying a flow expansion unit with wet vapour or liquid working medium can cause it to malfunction, reduce efficiency, and even fail. On the other hand, the study showed that the maximum efficiency of the PK70-type rotodynamic pump operating in the micro-ORC system with and without regeneration was 11.7% and 14.7%, respectively. This was due, among other factors, to internal losses in the pump, which increased the energy consumption of the pump. The HFE-7100 medium has approximately 1.5 times the density of water, and kinematic viscosity is more than twice as low.

A study conducted by Mathias et al. [71] on an ORC system with R123 medium showed that the gear pump was very energy-consuming, consuming about 2.2 kW. The researchers found that the duplex (positive-displacement) piston pump was less energy-consuming, with a power consumption of about 390 W and an isentropic efficiency of about 69% (including the motor).

On the other hand, the study [72] found that the HFE-7100 medium had virtually no lubricating properties and the use of rolling bearings caused the grease to be washed out, increasing the vibration level and ultimately damaging the expansion unit. HFE-7100 is a solvent primarily used in industry as a cleaning and washing agent. Therefore, using a piston pump and direct contact with the HFE-7100 medium would result in its damage. That is why, based on the above experience and literature data, an intermediate option was decided upon, namely the use of a diaphragm pump (type D/G-03, produced by HYDRA-CELLTM PUMP) in the ORC system and PE tests [25]. From the experimental tests carried out, it became apparent that after approximately 5 hours of PE operation with the HFE-7100 medium, the pump diaphragms were damaged (Fig. 1), and the lubricating oil from the diaphragm pump penetrated into the working medium cycle. It should be mentioned that at the time of selection and purchase, both the sellers of the working medium and the pumping engine declared the compatibility of the construction materials used for PE with the HFE-7100 medium. Moreover, the static chemical resistance to the HFE-7100 medium (the immersion test lasted 30 days) of the material samples (EPDM, Viton, Teflon), from which the pump diaphragms were made, was also confirmed by experimental tests conducted at the Institute of Fluid-Flow Machinery of the Polish Academy of Sciences (IFFM PAS) in Gdańsk.

Thus, during these tests, it was demonstrated that the material used from the pump diaphragms lacks resistance to the HFE-7100 liquid under varying dynamic loads, rendering PE unsuitable for use in the ORC system together with the diaphragm pump. It should be emphasised that there is currently a shortage of such studies and data in both the thematic literature and pump manufacturers' databases. That is why it is worth bearing in mind that the use of new working mediums that have not been fully tested brings many uncertainties to both the design and experimental testing of the components (i.e. PE) of an ORC system. It must then be assumed that the new working medium can be one of the causes of damage to the seals of the machines and their components and cause an increase in internal leakage in these devices [49,38], which, consequently, can lead to a reduction in their functionality and efficiency.

Research was also conducted with the HFE-7100 medium of a prototype Roto-Jet pump with a nominal rotational speed of 8000 rpm, a flow rate of 0.3 m^3/h and a specific speed of 2.19, which was designed and built at IFFM PAS, in Gdańsk [49]. The study showed that superheating of the working medium before entering the expansion valve was only achieved at a few points in the ORC system without regeneration, whereas in the system with regeneration, the HFE-7100 medium was in the wet vapour region. It was determined that the experimental results deviated to a significant extent (approximately 21%) from the design assumptions, analytical calculations, and 3D numerical calculations performed based on classical computational models [49]. Detailed analyses of the test results obtained showed that the working medium databases implemented in the computational models were incorrect. As it turned out, the properties of the mediums implemented in the commercial calculation programs, such as Engineering Equation Solver (EES) or Aspen Plus, commonly used in engineering calculations, differ significantly from the data obtained through experimental studies. For the HFE-7100 medium, for example, the maximum difference in kinematic viscosity (at 0°C) between the experimental data of Rausch et al. [73] and the data obtained from the EES program was approximately 32%. The same is true of the working medium database, e.g. REFPROP 9.1, which does not contain complete data on the thermophysical and physicochemical properties of the working medium HFE-7100. On the other hand, manufacturers of working mediums typically provide physicochemical data in their catalogues for only a single point, for normal or standard conditions (at 25°C and 1013.25 hPa). That is why ongoing efforts are being made to create reliable databases for new working mediums [74]. It should be borne in mind that the working mediums adopted for ORC systems repeatedly have a completely different application predicted by the manufacturer, as mentioned above.

To recapitulate, it can be stated that the rationale for conducting PE tests with a gear pump was driven, among other factors, by the uncertainty and lack of complete knowledge of the HFE-7100 medium used in the ORC system. Based on previous experience with this medium, it was necessary to investigate the PE under real operating conditions in a microsystem. This was due, among other factors, to the necessity of establishing the chemical interaction of this medium with the pump's structural components, determining the performance characteristics of the pump operating in the micro-ORC system, and filling the literature gap in this area. That is why this question is of interest both in terms of content and research. On the other hand, one

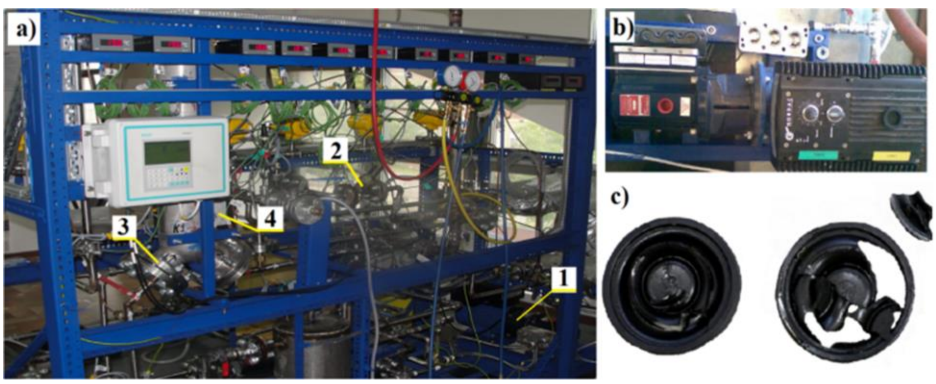

Fig. 1. a) ORC test rig, b) dismounted diaphragm pumping engine, c) damaged diaphragms; 1 – diaphragm pumping engine, 2 – expansion valve, 3 – regenerator, 4 – evaporator [25].

of the objectives of this study was to determine whether and to what extent the pumping engine can operate with the low-boiling liquid HFE-7100 in the micro-ORC system, and if so, what the actual operating characteristics of PE are.

3. Test bench

A study on a PE with a gear pump was conducted in a micro-CHP ORC system, a diagram and photograph of which are shown in Figs. 2 and 3, respectively. The micro-ORC system ultimately operates in conjunction with a 2.5 kW$_e$ micro turbogenerator (MTG) [75] powered by the vapour of the HFE-7100 working fluid [21]. The basic physicochemical parameters of the low-boiling fluid HFE-7100 are listed in Table 1. It should be noted that HFE-7100 is a dry working medium, as shown in the T-s diagram (Fig. 4). In view of the above, the PE should ensure nominal operating parameters for MTG, among others:

- mass flow rate (m_{nom}) – 0.17 kg/s,
- nominal vapour differential pressure in the microturbine (Δp_{nom}) – 1000 kPa,
- minimal vapour differential pressure in the microturbine (Δp_{min}) – 450 kPa.

The test rig used for the research on the PE consisted of three cycles: the heating cycle, the HFE-7100 working fluid cycle and the cooling cycle. A prototype two-module induction heater with a nominal power of 2 × 24 kW$_e$ was used to heat the thermal oil. The vapour of the working fluid from the expansion valve (EV) was directed successively to the condenser and then to the tank from which the PE was fed. The thermal oil was directed to the evaporator after being heated to a set temperature. A plate heat exchanger with a heat exchange surface area of 4.1 m^2 was used as an evaporator. The HFE-7100 working fluid, pumped by the PE, vaporised while flowing through the evaporator. It was then directed to the EV, which simulated MTG operation. The EV was used to throttle the flow of the working fluid and thus constituted the load for the tested PE. A plate heat exchanger with a heat exchange surface area of 3.2 m^2 was used as the condenser.

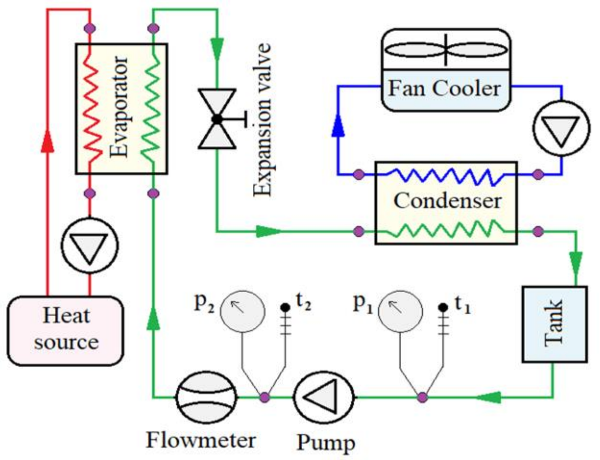

Fig. 2. Simplified diagram of a micro-ORC system: t_1 and t_2 – temperature measurement points at the pump inlet and outlet, p_1 and p_2 – pressure measurement points at the pump inlet and outlet.

Table 1. Selected physicochemical properties of the HFE-7100 working fluid at a temperature of 25°C and atmospheric pressure [21].

Properties	Values	Units
Boiling Point	61	°C
Liquid Density	1510	kg/m^3
Dynamic Viscosity	0.61	mPa s
Specific Heat	1183	J/kg K
Surface Tension	0.0136	N/m

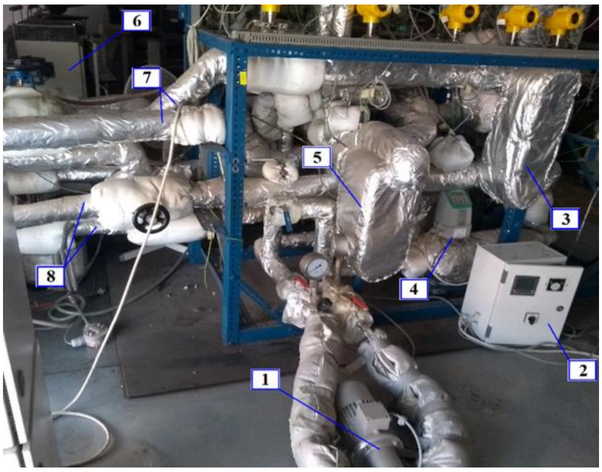

Fig. 3. Micro-ORC power plant test rig: 1 – pumping engine, 2 – frequency converter connected to the PE drive, 3 – evaporator, 4 – Coriolis mass flowmeter, 5 – condenser, 6 – control and regulation module for the induction heater, 7 – heating cycle piping, 8 – cooling cycle piping.

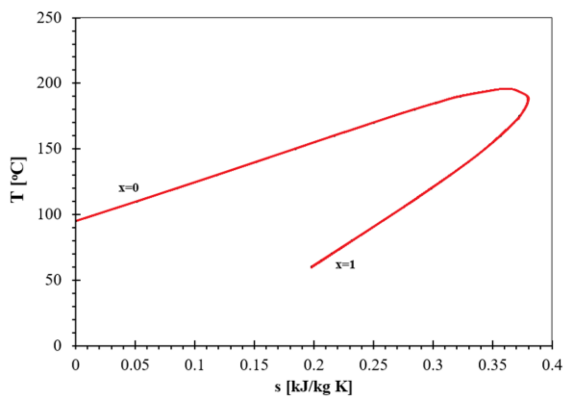

Fig. 4. T-s diagram of the HFE-7100 working medium.

The heat from the condenser on the working fluid side was dissipated using a 50 kW$_t$ fan cooler. In the fan cooler, a 40% solution of propylene glycol in distilled water was used as the working fluid.

3.1. Pumping engine

The tested PE was a commercial design that consisted of a gear pump (1.1), which was connected to an electric drive (1.3) via a magnetic coupling (1.2), as shown in Fig. 5. The technical data and operating parameters of the gear pump and electric drive are provided in Table 2.

Table 2. Selected technical data of PE (according to manufacturer's data).

Gear pump		Electric drive	
Manufacturer	Scherzinger	Manufacturer	Küenle
Type	gear	Type	synchronous
Model	4030-450-DM 075	Model	KTENW 80 K2 KT
Displacement	4.5 cm^3/rev	Class of construction	IE2
Maximum differential pressure	14 bar	Efficiency	77.4%
Maximum flow rate	15.75 l/min	Power rating	750 W
Maximum rotational speed	3,500 rpm	Rotational speed	3,000 rpm
Outer diameter of the gear wheel	25 mm	Rated voltage	230/400 V
Pitch diameter of the gear wheel	20 mm	Rated current	3.0/1.7 A
Inner diameter of the suction port	14.5 mm	Frequency	50 Hz
Inner diameter of the discharge port	14.5 mm	cos φ	0.80
Temperature range	from -20°C to +130°C	Insulation class	F
Maximum inlet pressure	100 bar	Ingress Protection code	IP55

The PE was connected to the micro-ORC system with the help of corrugated pipes (9,10) made of stainless steel. Manovacuometers (11,12) and shut-off valves (13,14) were fitted to the suction and discharge piping. The rotational speed of the gear pump was controlled by varying the frequency of the motor power supply using an inverter of the type SV015iG5A-4, manufactured by LS Electronics.

3.2. Test apparatus and measurement errors

K-type thermocouples with a diameter of 0.5 mm were used to measure the temperature of the working fluid before and after the pumping engine. On the other hand, pressure transducers and manovacuometers were used to measure pressures. The flow rate of the working fluid was measured using a Coriolis flowmeter (Fig. 2). The schedule and specifications of the measuring apparatus used for the PE tests are included in Table 3.

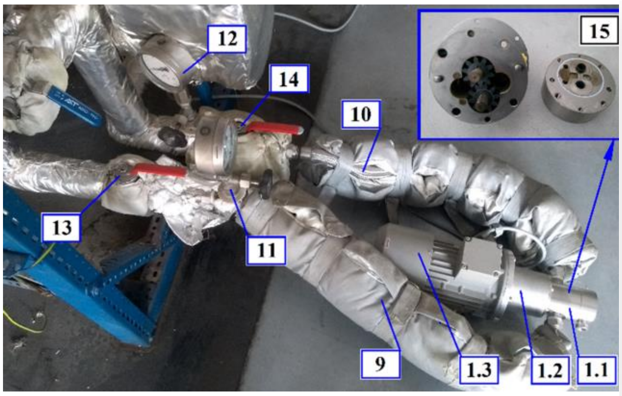

Fig. 5. Photograph of the PE on the test rig: 1.1 – gear pump, 1.2 – magnetic coupling, 1.3 – electric drive, 9 – pump supply pipe, 10 – pipe at the outlet of the gear pump, 11 and 12 – analogue manovacuometers fitted to the suction and discharge piping, respectively, 13 and 14 – shut-off valves fitted to the suction and discharge piping, respectively, 15 – the inside of the gear pump housing.

The standard uncertainties of the dimensionless numbers Re and Eu were 0.8% and 0.5%, respectively, as calculated from the relation (1):

$$u(k) = \left(\Delta k/\sqrt{3}\right) \cdot 100\%. \quad (1)$$

where: Δk – maximum uncertainty.

Table 3. Test apparatus and measurement sensors.

Instrument: type/model	Manufacturer	Range	Accuracy
Thermocouple: K-type, Class 1	Czaki Thermo-Product	-40°C – 600°C	± 0.0040·|t| [°C]
Pressure transducer: type NPXA, Class 0.1	Peltron	0 – 16 bar	± 0.1% MR
Analogue mano-vacuometer: Class 1.0	Wika	0 – 16 bar	± 0.16 bar MV
Coriolis mass flowmeter: model Sitrans FC, type Mass 2100	Siemens	0 – 5,600 kg/h	± 0.1% MV
Meter of network parameters, type ND20	Lumel	0.002 – 1.200 A 0.010 – 6.000 A	± 0.2% MR
		5 – 480 V	± 0.5% MR
		-1.65 – 1.65 kW	± 0.5% MR
		-1.65 – 1.65 kVar	± 0.5% MR
		1.4 – 1.65 kVA	± 0.5% MR

MR – measurement range, MV – measurement value

Manovacuometers were used as additional measuring instruments to monitor pressure during the start-up of the ORC system. A meter of network parameters, of the type ND20, was used to measure the electric power consumed by the pumping engine drive. All measured quantities were recorded and archived by a measurement system from National Instruments (NI). A program specifically written in the LabView environment was utilised to record, archive, and visualize the measurement data. All measured quantities were recorded every 1 second on an NI measurement computer.

4. Methodology and research procedure

The research methodology of the PE is shown in Figure 6. The PE was tested at three preset rotational speeds: n_1 = 1000 rpm, n_2 = 1500 rpm, and n_3 = 2000 rpm. At each preset rotational speed, the PE was tested in two temperature ranges (R1 and R2) of the HFE-7100 working fluid, which were measured at the pump supply. The temperature waveforms of the HFE-7100 working fluid measured at the pump supply depending on the pump's differential pressure for the preset rotational speeds of the pump are shown in Fig. 7.

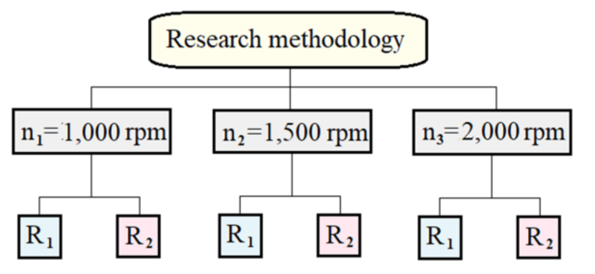

Fig. 6. Metrology of PE testing.

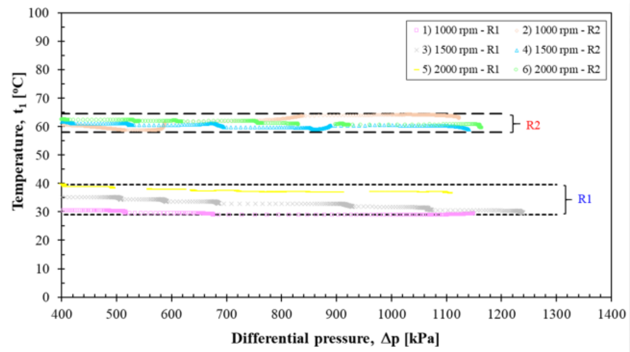

Fig. 7. Temperature ranges of HFE-7100 versus differential pressure of the pump unit.

The first temperature range (R1) of the HFE-7100 working fluid (t_1 – Fig. 7) covered the range from 29°C to 39°C, and the second (R2) from 58°C to 64°C. In R1, the average temperature value of HFE-7100 was t_{av1}=34 ±5 °C, and in R2, it was t_{av2}=61 ± 3 °C. It should be emphasised that the boiling point of HFE-7100 at atmospheric pressure is 61 °C. That is why the working fluid with a temperature of 61 °C directed from the tank to the pump's suction channel should have a pressure higher than atmospheric to avoid cavitation. The pressure of the working fluid behind EV was regulated by a condenser heat removal system (Fig. 2).

The temperature ranges R1 and R2 were determined based on the technical capabilities of the heat removal system for the heat exchangers (evaporator and condenser). The tolerances in the average temperature values of HFE-7100, and thus the ranges R1 and R2, were, among other things, due to the limited possibilities of regulating the operating parameters of the cycles as a result of the high thermal inertia of the ORC system. Therefore, maintaining small temperature tolerances with the required minimum differential pressure (450 kPa) of the working fluid for the preset rotational speeds of the pump was rendered difficult, particularly in the R2 range.

That is why the proposed research methodology had two principal objectives. Firstly, to verify: At what operating parameters will PE ensure nominal operating conditions for MTG? Secondly, at what rotational speed levels (n_1, n_2, n_3) and preset temperature levels (R1, R2) of the low-boiling fluid HFE-7100 will the efficiency of PE be the highest?

4.1. Research procedure

The research procedure involved setting the power and oil temperature on the control panel of the electric induction heater, which were 30 kW$_t$ and 200°C, respectively, under the nominal operating conditions of MTG. Then, the oil pump was started, and a verification of the correct operation of the measuring apparatus and indications of measuring instruments was performed. After positive tests, the electric induction heater was put into operation. The rotational speed of the oil pump, and thus the value of the oil flow rate in the heating cycle, was regulated using an inverter.

The system's heating process was carried out until the thermal oil temperature reached approximately 100°C. At that time, the fan cooler and glycol pump were started, and the proper operation of the measurement system in this cycle was checked. Then, the process of starting the working fluid cycle, in which the tested PE was mounted, was initiated. Using an inverter, the present rotational speed (i.e., n_1, n_2 or n_3) of the PE, and thus the flow rate value of the HFE-7100 working fluid, was set. At this stage of the research, the expansion valve was fully open. At that time, the forcing pressure value of the working fluid was approximately 120 kPa.

For this value of working fluid pressure and a thermal oil temperature of about 100°C, the process of complete evaporation of HFE-7100 in the evaporator occurred. By varying the flow rate of the glycol solution, the average temperature of the working fluid, t_{av1} or t_{av2}, was regulated to fall within the present range of R1 or R2. Control of the flow rate of the glycol solution in the cooling cycle was realised by changing the rotational speed of the glycol pump using an inverter. Once the microsystem was warmed up and the set temperature (t_{av1} or t_{av2}) was within the tolerance limit (R1 or R2), the process of loading PE commenced. PE was loaded by means of changing the degree of opening of the expansion valve, which made it possible to determine the so-called choking characteristics. The same procedure was used for each preset rotational speed of PE.

5. Calculation methods

The effective (useful) delivery head of the pump H_u was calculated from Eq. (2):

$$H_u = \Delta p / g\rho. \quad (2)$$

The volumetric efficiency of the pump was calculated from Eq. (3):

$$\eta_{vol} = (m_r / m_{th})\ 100\%. \quad (3)$$

The value of the theoretical flow rate of the pump was calculated from Eq. (4):

$$m_{th} = \rho V f. \quad (4)$$

The specific speed of the pump was calculated from Eq. (5):

$$\Omega_s = \omega q^{1/2} / (gH)^{3/4}. \quad (5)$$

The delivery head of the pump was calculated from Eq. (6):

$$H = p_2 / g\rho. \quad (6)$$

The net (effective) power of the pump, P_u, was calculated from Eq. (7):

$$P_u = q\Delta p. \quad (7)$$

The efficiency of the pumping engine, η_{PE}, was calculated from Eq. (8), which has the form:

$$\eta_{PE} = (P_u / N_e)\ 100\%. \quad (8)$$

As mentioned earlier, one of the essential parameters required from PE is an adequate differential pressure (Δp) of the working fluid. That is why the dimensionless parameter Euler number (Eu) was introduced into the analysis, which was calculated from Eq. (9):

$$Eu = \Delta p / \rho w^2. \quad (9)$$

The flow velocity was calculated from Eq. (10):

$$w = q / (\pi d_i^2 / 4). \quad (10)$$

The nature of flow of the working fluid through the pump was determined based on the Reynolds number (Re), which was calculated from Eq. (11):

$$Re = w\rho d_i / \mu. \quad (11)$$

6. Results and discussions

As mentioned earlier, the differential pressure in the pump (Δp) is one of the essential parameters required for the correct operation of expansion microunits. That is why the elaborated experimental performance characteristics of PE are presented as a function of differential pressure, among others, as detailed in Section 6.1. The efficiency characteristics of the pump and PE are discussed in Section 6.2. On the other hand, an analysis of PE operation in the ORC system based on dimensionless numbers is provided in Section 6.3.

6.1. Analysis of the effect of differential pump pressure

Figure 8 shows that with an increase in the differential pressure value (Δp), the useful delivery head of the pump (H_u) increased. It was observed that the pump rotational speed did not have a fundamental impact on the value of the useful delivery head of the pump.

This manifested itself in the fact that the measurement data labelled 1, 3 and 5 (see Fig. 8), being in the R1 temperature range, could be approximated by a single line. Similarly, in the R2 temperature range, the measurement data (labelled 2, 4 and 6 in Fig. 8) aligned along a single approximation line (broken line). Furthermore, it was found that irrespective of the temperature of the working fluid, the useful delivery head of the pump increased with the rise in the differential pressure generated by the pump. On the other hand, an increase in the temperature of the working fluid at the same differential pressure resulted in a further increase in the value of the useful delivery head (ΔH_U) of the pump. This was manifested by the increase in the slope value of the approximating straight lines.

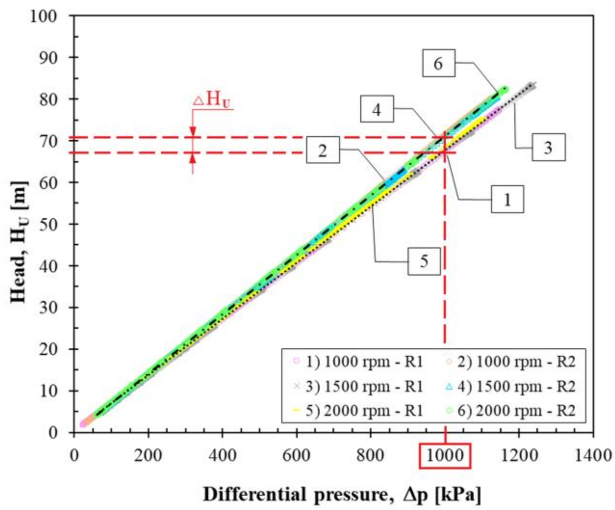

Fig. 8. Useful delivery head of the pump versus differential pressure.

Figure 9 shows the electric power (N_e) consumed by the PE drive versus differential pressure. The study reveals that, regardless of the temperature of the working fluid, the electric power consumed by the PE drive is directly proportional to the differential pressure of the pump.

It was determined that as the rotational speed and the temperature of the working fluid increase, the power consumed by the pump increases. In the analysed case, for this same value of differential pressure and at a pump rotational speed of 1000 rpm, the temperature increase from R1 to R2 resulted in an increase in the electric power ($\Delta N_{e\text{-}n1}$) consumed by the pump drive by 26 W_e. On the other hand, at a rotational speed of

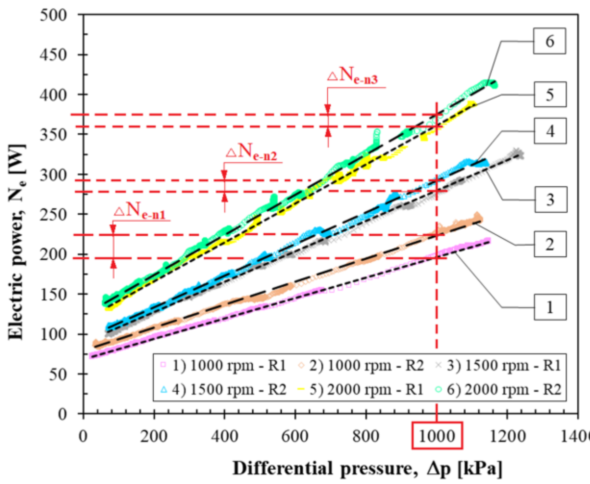

Fig. 9. Electric power consumed by the PE drive versus differential pressure.

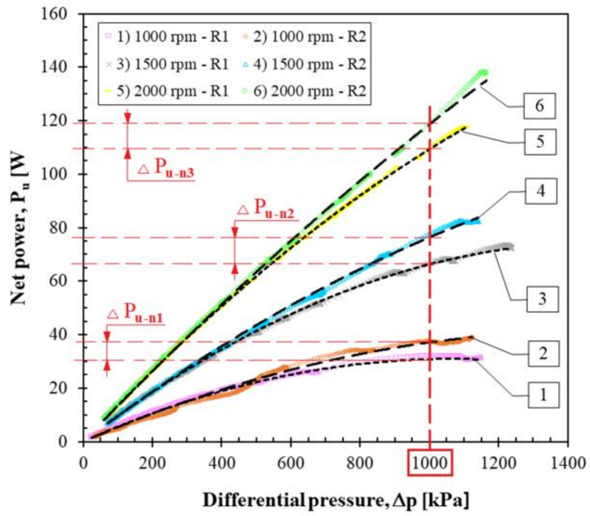

Fig. 10. Dependence of the net pump power on the differential pressure.

1500 rpm, an increase in the consumed electric power ($\Delta N_{e\text{-}n2}$) of approximately 18 W_e was recorded. In the case when the pump rotational speed was 2000 rpm, the increase in electric power consumption ($\Delta N_{e\text{-}n3}$) by the pump drive was approximately 16 W_e. This means that as the rotational speed increases, the electric power consumption by the PE drive decreases (Fig. 9). Table 4 includes the values of power consumed by the PE drive for preset pump rotational speeds and a differential pressure of 1000 kPa.

Table 4. Operating parameters of PE for a differential pressure of 1000 kPa and preset pump rotational speeds.

Characteristics	Parameters	Pump rotational speed			Units
		1000	1500	2000	rpm
$H_u(\Delta p)$	R1	67	67	67	m
	R2	71	71	71	m
	ΔH_u	*6*	*6*	*6*	%
$N_e(\Delta p)$	R1	199	278	359	W
	R2	225	295	375	W
	ΔN_e	*13.1*	*6.1*	*4.4*	%
$P_u(\Delta p)$	R1	31	66	110	W
	R2	37	77	120	W
	ΔP_u	*19.3*	*16.7*	*9.1*	%

Figure 10 shows that the effective power of the pump increases with increasing differential pressure and rotational speed of the pump. It was observed that above a differential pressure of about 450 kPa, the temperature of the working fluid has a fundamental impact on the effective power of the pump. It also results from this that at the first ($\Delta P_{u\text{-}n1}$), second ($\Delta P_{u\text{-}n2}$) and third ($\Delta P_{u\text{-}n3}$) rotational speeds, the increases in the effective power of the pump were 6 W, 9 W, and 10 W, respectively. This means that at a constant differential pressure, there was an increase in the average effective power of the pump as the temperature of the working fluid increased. As mentioned earlier, the second necessary condition for the use of PE in the micro-ORC system and the correct operation of MTG is to ensure an adequate flow rate of the working fluid.

6.2. Analysis of the effect of ORC system operating parameters on PE efficiency

As mentioned earlier (Section 3), the value of the nominal flow rate of HFE-7100 in the 2.5 kW_e MTG is approximately 0.17 kg/s. Moreover, the pump is required to have the highest possible efficiency. That is why Fig. 11 shows the dependence of the volumetric efficiency of the pump on the flow rate of the

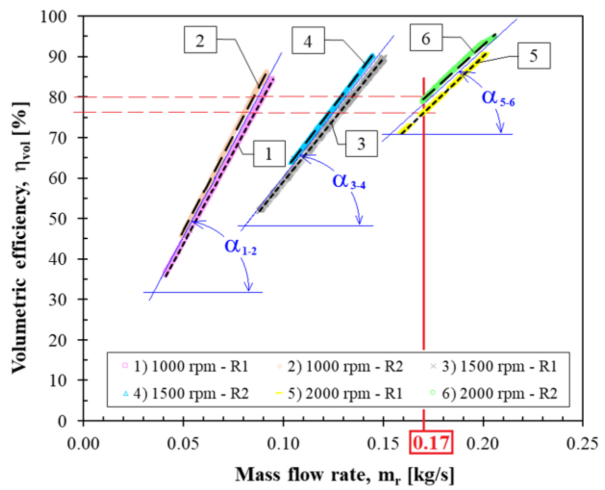

Fig. 11. Dependence of pump volumetric efficiency on the HFE-7100 flow rate.

working fluid. The study (Fig. 11) reveals that as the pump rotational speed increases, the slopes (α) of the straight lines approximating the pump efficiency versus the working fluid flow rate decrease. That is why, as the pump rotational speed increases, the characteristics are steeper. For example, for a rotational speed of 1000 rpm, the average value of the angle ($\alpha_{1\text{-}2}$) within the temperature range R1 and R2 was approximately 62° (Fig. 11). For a rotational speed of 1500 rpm, the average value of the $\alpha_{3\text{-}4}$ angle was approximately 52°. On the other hand, for a pump rotational speed of 2000 rpm, the value of the $\alpha_{5\text{-}6}$ angle was approximately 42°.

It has been established that a 500 rpm change in the rotational speed of the pump results in a change of the inclination angle of the straight line approximating the volumetric efficiency of the pump by 10°. That is why, at low rotational speeds (lines 1 and 2), a small change in the flow rate of the working fluid results in a large change in the volumetric efficiency of the pump.

The study reveals that an increase in the temperature of the working fluid results in an increase in the volumetric efficiency of the pump. For example, for a flow rate of 0.17 kg/s (Fig. 11) in the R1 temperature range, the average value of the pump volumetric efficiency was approximately 76%, and in the R2 range, it was approximately 80%. Furthermore, it can be seen from Fig. 11 that achieving an HFE-7100 flow rate equal to 0.17 kg/s is only possible with a pump rotational speed of at least 2000 rpm (lines 5 and 6).

Figure 12 shows that an increase in the rotational speed of the pump resulted in an increase in the efficiency of the PE. It has been established that for each value of speed and working fluid temperature, there exists an optimum effective power value for the pump at which the efficiency of PE is maximum. For a pump rotational speed of 1000 rpm, in the R1 temperature range, the maximum PE efficiency of approximately 17.0% was achieved with an effective power of 25 W. On the other hand, an increase in the HFE-7100 temperature from R1 to R2 resulted in an increase in PE efficiency to 17.2%, which was obtained with an effective power of 30 W.

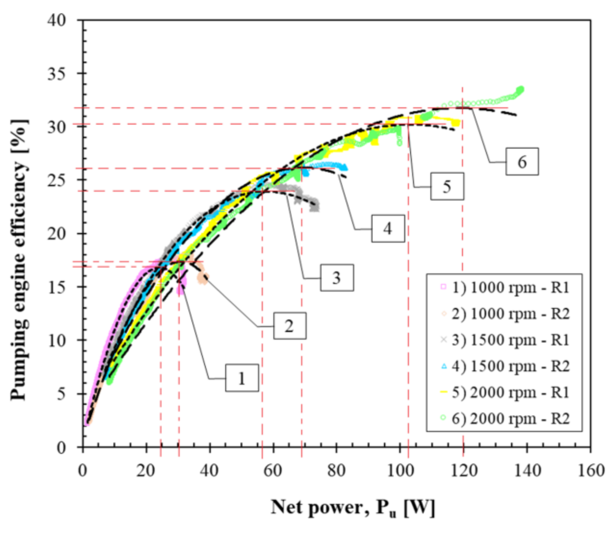

Fig. 12. Effect of the effective power of the pump on the efficiency of PE.

Similarly, at pump rotational speeds of 1500 rpm and 2000 rpm, the increase in temperature resulted in an increase in the efficiency of PE. The maximum efficiencies of PE at a rotational speed of 1500 rpm for the temperature ranges R1 and R2 were 19.0% and 26.0%, respectively. On the other hand, at a rotational speed of 2000 rpm, the efficiency maxima for the R1 and R2 ranges were 30.2% and 31.8%, respectively.

These efficiency values were obtained at the effective powers of the pump, which were 103 W and 120 W, respectively. It is worth noting that for a pump rotational speed of 2000 rpm (at the MTG's nominal operating point), regardless of the HFE-7100 temperature, the volumetric efficiencies of the pump were approximately 60% higher (Fig. 12) than the PE efficiencies obtained. This means that not only the pump but also the efficiencies of the drive and magnetic coupling have a very significant impact on the efficiency of PE. At a nominal rotational speed of 3000 rpm, the efficiency of the electric drive is approximately 77%. That is why PE operation below the rated rotational speed of the electric drive resulted in significant losses.

6.3. Analysis of PE operation in terms of dimensionless numbers

Figure 13 shows that the temperature of the working fluid has a fundamental impact on the value of the Reynolds number (Re). It was determined that at the nominal flow rate of the MTG (i.e., 0.17 kg/s), in the HFE-7100 temperature range R1, Re was approximately 30 000. On the other hand, in the R2 range of working fluid temperatures, the Re number was approximately 40 800. As can be seen in Fig. 13, the value of the Re number over the entire investigated range of temperatures (R1 and R2) and pump rotational speeds (n_1 to n_3) was above 3000. This means that the flow of the working fluid was turbulent.

Furthermore, the study reveals that the measurement data obtained in the R1 temperature range over the entire range of rotational speeds could be approximated by a single line. On the

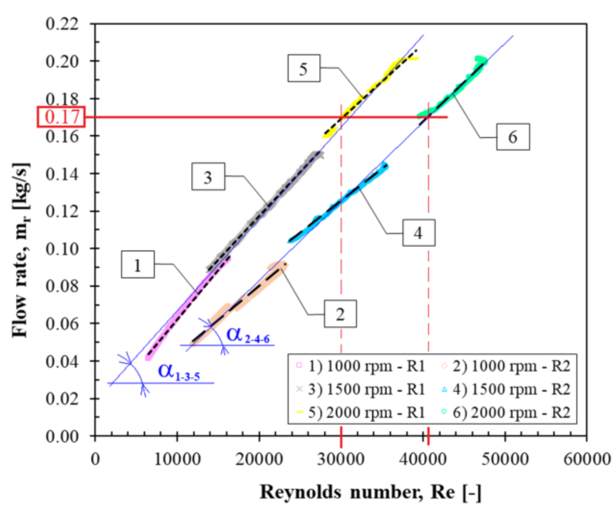

Fig. 13. HFE-7100 flow rate versus Re number.

other hand, the angle value of the slope ($\alpha_{1\text{-}3\text{-}5}$) of this straight line was approximately 48°. In the case when the working fluid temperatures were in the R2 range, the angle value ($\alpha_{2\text{-}4\text{-}6}$) was approximately 44°. That is why it can be deduced that as the temperature of the working fluid increased, the value of the Reynolds number increased.

Figure 14 shows that the value of the working fluid temperature and Re have a fundamental impact on the volumetric efficiency of the pump. It was observed that as the working fluid temperature and pump rotational speed increase, the characteristics of the pump efficiency shift to the right towards larger values of the Re number.

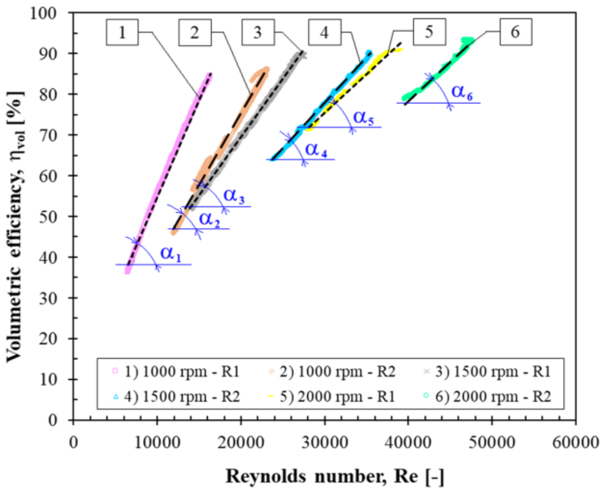

Fig. 14. Dependence of pump volumetric efficiency on Re number.

Furthermore, as the temperature increased, the characteristics were flatter, which manifested itself as a reduction in the value of the slope of the approximating straight lines. For a pump rotational speed of 1000 rpm, the inclination angle of the function (α_1) in the R1 temperature range was approximately 67°. In the same temperature range and at a rotational speed of 1500 rpm, the α_3 inclination angle was approximately 53°, and at a rotational speed of 2000 rpm, the value of the α_5 angle was approximately 44°. On the other hand, in the R2 temperature range, the values of angles α_2, α_4 and α_5 (see Fig. 14) corresponding to the pump rotational speeds of 1000 rpm, 1500 rpm and 2000 rpm were 60°, 47° and 42°, respectively.

That is why it can be deduced that at low pump rotational speeds and low working fluid temperatures, small changes in the Reynolds number result in significant changes in the volumetric efficiency of the pump.

Figure 15 shows the dependence of the electric power consumed by the PE drive on the specific speed. In addition, the study reveals that irrespective of the pump rotational speed, a change in working fluid temperature from R1 to R2 caused the pump power curves to intersect at the so-called 'characteristic points' (Fig. 15). At a pump rotational speed of 1000 rpm, the characteristics intersected at point A, where the specific speed

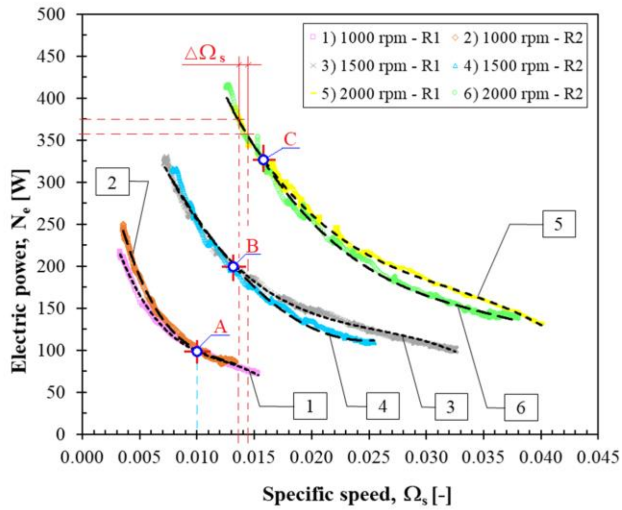

Fig. 15. Dependence of the electric power consumed by the PE drive on specific speed.

was approximately 0.010. It was observed that to the right of point A, power curves 1 and 2 coincided.

That is why the temperature of the medium had no effect on the course of the power curves. On the other hand, to the left of point A, an increase in the temperature of the working fluid resulted in an increase in the power consumed by the pump drive. The maximum increase in power consumed at a rotational speed of 1000 rpm was approximately 13.6%, and the specific speed value was approximately 0.0035. At a rotational speed of 1500 rpm, the performance curves of the pump intersected at point B.

As the pump rotational speed increased, the characteristic points shifted to the right towards higher specific speed values. It was determined that a 500 rpm increase in pump rotational speed resulted in a 0.003 increase in the value of Ω_s. It was observed that at rotational speeds of 1500 rpm and 2000 rpm to the left of characteristic points B and C, the power curves overlapped. This means that, in this area, the impact of the working fluid temperature on the course of the pump's performance curves was small. On the other hand, to the right of points B and C, an increase in the temperature of the fluid from R1 to R2 resulted in a decrease in the electric power consumption of the pump drive.

It should be noted that at MTG's nominal operating parameters (Δp=1000 kPa and m_r=0.17 kg/s), the difference in specific speed ($\Delta\Omega_s$) due to temperature changes from R1 to R2 was approximately 0.001. Therefore, at the MTG's nominal operating point, the value of Ω_s will be 0.014 ± 0.0005 regardless of the working fluid temperature.

Figure 16 shows the effect of specific speed on the effective power of the pump. It was observed that, as a result of the increase in the rotational speed, the performance curves shifted to the right towards higher specific speed values. On the other hand, irrespective of the rotational speed and working fluid temperature, the effective power value of the pump decreased as the specific speed increased. It has been determined that the working fluid temperature has a fundamental impact on the value of the pump's effective power.

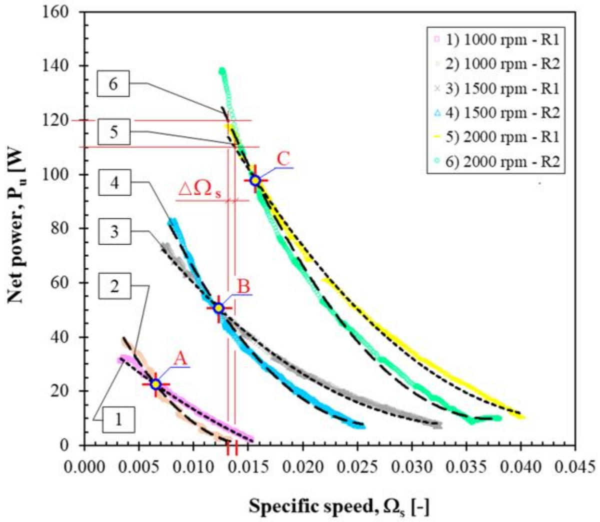

Fig. 16. Effect of specific speed on the effective power of the pump.

To the left of point A, the increase in working fluid temperature from R1 to R2 resulted in an increase in the effective power of the pump. In the R2 range, the maximum effective power value was approximately 40 W and it was approximately 23% higher than that obtained in the R1 temperature range. On the other hand, to the right of point A, an increase in temperature resulted in a decrease in the effective power value. In the R1 temperature range, with Ω_s equal to 0.014 and a rotational speed of 1000 rpm, the effective power was approximately 7.5 W, and in the R2 range, it was three times lower.

Similarly, at higher rotational speeds in the R1 temperature range and for the same Ω_s value, higher effective powers were obtained than in the R2 range. The study reveals that characteristic points B and C, determined on the effective power curves at rotational speeds of 1500 rpm and 2000 rpm respectively, were noted successively at specific speeds of approximately 0.0135 and 0.0165, respectively.

Figure 16 shows that to the left of points B and C, higher effective power values of the pump were obtained in the R2 temperature range. That is why, as the rotational speed increased, the differences in effective power decreased due to changes in the temperature of the working fluid. On the other hand, at the MTG's nominal operating point, a change in HFE-7100 temperature from R1 to R2 resulted in an increase in specific speed from approximately 0.013 to 0.014.

As mentioned earlier, an essential parameter required from PE is to ensure adequate differential pressure in the ORC system. On the other hand, in accordance with Eq. (9), differential pressure is a component of the Euler number (Eu). That is why Fig. 17 shows the characteristics of the power consumed by the pump drive versus the Eu number.

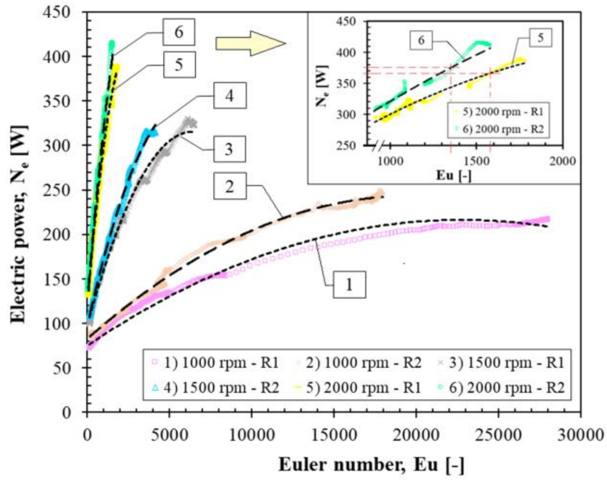

Fig. 17. Effect of the Euler number on the electric power consumed by the PE drive.

As can be deducted from Fig. 17, the value of the Eu number decreases with increasing pump rotational speed and working fluid temperature. As a result, the performance curves of PE were steeper. Therefore, a small increase in the value of the Eu number resulted in significant electric power consumption by the PE drive. On the other hand, at the MTG's nominal operating point in the temperature ranges R1 and R2, the values of the Eu numbers were 1350 and 1580, respectively. The study reveals that, at low rotational speeds, the electric power consumption by the pump drive in the R2 temperature range is greater than when operating in the R1 range. To recapitulate, it can be stated that irrespective of the pump rotational speed, an increase in the temperature of the working fluid results in a higher electric power consumption by the pump drive.

6. Conclusions

The study reveals that an increase in working fluid temperature, differential pressure in the pump and rotational speed results, firstly, in an increase in effective power. Secondly, it causes an increase in the delivery head of the pump. Thirdly, it results in an increase in the electric power consumed by the pumping engine drive. The study reveals that an increase in the temperature of the HFE-7100 working fluid results in an increase in the volumetric efficiency of the pump. For example, at a rotational speed of 2000 rpm, an increase in the average temperature of the working fluid from 34°C to 61°C resulted in an increase in the volumetric efficiency of the pump from 76% to approximately 80%. Moreover, it was stated that for each value of pump rotational speed and working fluid temperature, there exists an optimum value of the effective power of the pump at which the efficiency of the pumping engine reaches the maximum value.

Based on the study, it was established that the maximum efficiency of the pumping engine, approximately 32%, was achieved at a rotational speed of 2000 rpm. At the same time, it was observed that, regardless of the change in the temperature of the working fluid, the efficiency of the pumping engine was, on average, about 60% smaller than the volumetric efficiency of the pump.

Acknowledgements

This study was conducted as part of the statutory works of the Institute of Fluid-Flow Machinery of the Polish Academy of Sciences (IFFM PAS) in Gdańsk and part of the TechRol project financed by the National Centre for Research and Development (NCBR) (grant agreement No. BIOSTRATEG3/344128/12/NCBR/2017).

References

[1] Hasan, A., Mugdadi, B., Al-Nimr, M.A., & Tashtoush, B. (2022). Direct and indirect utilization of thermal energy for cooling generation: A comparative analysis. *Energy*, 238 (Part C), 122046. doi: 10.1016/j.energy.2021.122046

[2] Kruk-Gotzman, S., Ziółkowski, P., Iliev, I., Negreanu, G-P., & Badur, J. (2023). Techno-economic evaluation of combined cycle gas turbine and adiabatic compressed air energy storage integration concept. *Energy*, 266, 126345. doi: 10.1016/j.energy.2022.126345

[3] Montazerinejad, H., & Eicker, U. (2022). Recent development of heat and power generation using renewable fuels: A comprehensive review. *Renewable and Sustainable Energy Reviews*, 165, 112578. doi: 10.1016/j.rser.2022.112578

[4] Wei, J., Hua, Q., Yuan, L., Li, G., Wang, J., & Wang, J. (2023). A review of the research status of scroll expander. *Proceedings of the Institution of Mechanical Engineers, Part A: Journal of Power and Energy*, 237(1), 176–197. doi: 10.1177/09576509221109245

[5] Minea, V. (2014). Power generation with ORC machines using low-grade waste heat or renewable energy. *Applied Thermal Engineering*, 69(1–2), 143-154. doi: 10.1016/j.applthermaleng.2014.04.054

[6] Di Battista, D., & Cipollone, R. (2023). Waste Energy Recovery and Valorization in Internal Combustion Engines for Transportation. *Energies*, 16, 3503. doi: 10.3390/en16083503

[7] Kaczmarczyk, T.Z. (2021). Experimental research of a small biomass organic Rankine cycle plant with multiple scroll expanders intended for domestic use. *Energy Conversion and Management*, 244, 114437. doi: 10.1016/j.enconman.2021.114437

[8] Jain, S.V., Patel, R.N. (2014). Investigations on pump running in turbine mode: A review of the state-of-the-art. *Renewable and Sustainable Energy Reviews*, 30, 841–868. doi: 10.1016/j.rser.2013.11.030

[9] Kottapallia, A. & Konijeti, R. (2022). Numerical and experimental investigation of nonlubricated air scroll expander derived from a refrigerant scroll compressor. *Frontiers in Heat and Mass Transfer*, 19(1), 1–11. doi: 10.5098/hmt.19.11

[10] Zhang, X., Wang, X., Cai, J., Wang, R., Bian, X., He Z., Tian, H., & Shu, G. (2023). Operation strategy of a multi-mode Organic Rankine cycle system for waste heat recovery from engine cooling water. *Energy*, 263 (Part E), 125934. doi: 10.1016/j.energy.2022.125934

[11] Gunawan, G., Permana, D.I., & Soetikno, P. (2023). Design and numerical simulation of radial inflow turbine of the regenerative Brayton cycle using supercritical carbon dioxide. *Results in Engineering*, 17, 100931. doi: 10.1016/j.rineng.2023.100931

[12] Li, X., Lv, C., Yang, S., Li J., Deng, B., & Qing, Li Q. (2019). Preliminary design and performance analysis of a radial inflow turbine for a large-scale helium cryogenic system. *Energy*, 167, 106–116. doi: 10.1016/j.energy.2018.10.179

[13] Liaw, K.L., Kurnia, J.C., Lai, W.K., Ong, K.Ch., Zar, M.A.B.M.A, Muhammad, M.F.B., & Firmansyah. (2023). Optimization of a novel impulse gas turbine nozzle and blades design utilizing Taguchi method for micro-scale power generation. *Energy*, 282, 129018. doi: 10.1016/j.energy.2023.129018

[14] Zhar, R., Allouhi, A., Ghodbane, M., Jamil, A., & Khadija, L.K. (2021). Parametric analysis and multi-objective optimization of a combined Organic Rankine Cycle and Vapor Compression Cycle. *Sustainable Energy Technologies and Assessments*, 47, 101401. doi: 10.1016/j.seta.2021.101401

[15] Kolasiński, & P., Daniarta, S. (2021). Sizing the thermal energy storage (TES) device for organic Rankine cycle (ORC) power systems. *MATEC Web of Conferences*, 345, 00018. doi: 10.1051/matecconf/202134500018

[16] Zhang, H-H., Zhang, Y-F., Feng, Y-Q., Chang, J-Ch., Chang, Ch-W., Xi, H., Gong, L., Hung, T-Ch., & Li, M-J. (2023). The parametric analysis on the system behaviors with scroll expanders employed in the ORC system: An experimental comparison. *Energy*, 268, 126713. doi: 10.1016/j.energy.2023.126713

[17] Milewski, J., & Krasucki, J. (2018). Comparison of ORC and Kalina cycles for waste heat recovery in the steel industry. *Journal of Power Technologies*, 97(4), 302–307.

[18] Alperen B., C., & Oğuz A. (2024). Numerical analysis-based performance assessment of the small-scale organic Rankine cycle turbine design for residential applications. *Thermal Science and Engineering Progress*, 51, 102626. doi: 10.1016/j.tsep.2024.102626

[19] Ziółkowski, P., Hyrzyński, R., Lemański, M., Kraszewski, B., Bykuć, S., Głuch, S., Sowiżdżał, A., Pająk, L., Wachowicz-Pyzik, A., & Badur, J. (2021). Different design aspects of an Organic Rankine Cycle turbine for electricity production using a geothermal binary power plant. *Energy Conversion and Management*, 246, 114672. doi: 10.1016/j.enconman.2021.114672

[20] Wang, R., Jiang, L., Ma, Z., Gonzalez-Diaz, A., Wang, Y., & Roskilly, A.P. (2019). Comparative Analysis of Small-Scale Organic Rankine Cycle Systems for Solar Energy Utilisation. *Energies*, 12(5), 829. doi: 10.3390/en12050829

[21] Kaczmarczyk, T.Z., & Żywica, G. (2022) Experimental study of a 1 kW high-speed ORC microturbogenerator under partial load. *Energy Conversion and Management*, 272, 116381. doi: 10.1016/j.enconman.2022.116381

[22] Peng, N., Wang, E., & Wang, W. (2023). Design and analysis of a 1.5 kW single-stage partial-admission impulse turbine for low-grade energy utilization. *Energy*, 268, 126631. doi: 10.1016/j.energy.2023.126631

[23] Witanowski, Ł., Klonowicz, P., Lampart, P., Klimaszewski, P., Suchocki, T., Jędrzejewski, Ł., Zaniewski, & D., Ziółkowski, P. (2023). Impact of rotor geometry optimization on the off-design ORC turbine performance. *Energy*, 265, 126312. doi: 10.1016/j.energy.2022.126312

[24] Ekwonu, M.C., Kim, M., Chen, B., Nasir, M.T., & Kim, K.C. (2023). Dynamic Simulation of Partial Load Operation of an Organic Rankine Cycle with Two Parallel Expanders. *Energies*, 16(1), 519. doi: 10.3390/en16010519

[25] Kaczmarczyk, T.Z. (2022). Thermal flow and electrical power research of ORC micro-cogeneration systems and their components. *Summary of Professional Accomplishments – Appendix No. 3 to the habilitation proceedings*. Gdańsk, Poland. https://www.imp.gda.pl/en/bip/postepowania-habilitacyjne/ [accessed: 3 Oct. 2023].

[26] Casari, N., Fadiga, E., Pinelli, M., Randi, S., & Suman, A. (2019). Pressure Pulsation and Cavitation Phenomena in a Micro-ORC System. *Energies*, 12(11), 2186. doi: 10.3390/en12112186

[27] Witanowski, Ł., Ziółkowski, P., Klonowicz, P., & Lampart, P. (2023). A hybrid approach to optimization of radial inflow turbine with principal component analysis. *Energy*, 272, 127064. doi: 10.1016/j.energy.2023.127064

[28] Fakeye, A.B., & Oyedepo, S.O. (2019). Designing Optimized Organic Rankine Cycles Systems for Waste Heat-to-Power Conversion of Gas Turbine Flue Gases. *International Conference on Engineering for Sustainable World. Journal of Physics: Conference Series*, 1378, 032097. IOP Publishing. doi: 10.1088/1742-6596/1378/3/032097

[29] Xi, H., Zhang, H., He, Y-L., & Huang, Z. (2019). Sensitivity analysis of operation parameters on the system performance of organic Rankine cycle system using orthogonal experiment. *Energy*, 172, 435–442. doi: 10.1016/j.energy.2019.01.072

[30] Fatigati, F., Vittorini, D., Wang, Y., Song, J., Markides ,C.N., & Cipollone, R. (2020). Design and Operational Control Strategy for Optimum Off-Design Performance of an ORC Plant for Low-Grade Waste Heat Recovery. *Energies*, 13(21), 5846. doi: 10.3390/en13215846

[31] Ziviani, D., Gusev, S., Lecompte, S., Groll, E.A., Braun, J.E., Horton, W.T., Broek, M., & De Paepe, M. (2017). Optimizing the performance of small-scale organic Rankine cycle that utilizes a single-screw expander. *Applied Energy*, 189, 416–432. doi: 10.1016/j.apenergy.2016.12.070

[32] Meng, F., Zhang, H., Yang, F., Hou, X., Lei, B., Zhang, L., Wu, Y., Wang, J., & Shi, Z. (2017). Study of efficiency of a multistage centrifugal pump used in engine waste heat recovery application. *Applied Thermal Engineering*, 110, 779–786. doi: 10.1016/ j.applthermaleng.2016.08.226

[33] Quoilin, S., Broek M., Declaye, S., Dewallef, P., & Lemort, V. (2013). Techno-economic survey of Organic Rankine Cycle (ORC) systems. *Renewable and Sustainable Energy Reviews*, 22, 168–186. doi: 10.1016/j.rser.2013.01.028

[34] Moradi, R., Habib, E., Bocci, E., & Cioccolanti, L. (2021). Component-Oriented Modeling of a Micro-Scale Organic Rankine Cycle System for Waste Heat Recovery Applications. *Applied Sciences.* 11(5), 1984. doi: 10.3390/app11051984

[35] Kaczmarczyk, T.Z., & Żywica, G. (2022). Experimental research of a micropower volumetric expander for domestic applications at constant electrical load. *Sustainable Energy Technologies and Assessments*, 49, 101755. doi: 10.1016/j.seta.2021.101755

[36] Huo, E., Xin, L., & Wang, S. (2022). Thermal stability and pyrolysis mechanism of working fluids for organic Rankine cycle: A review. *International Journal of Energy Research*, 46(14), 19341–19356. doi: 10.1002/er.8518

[37] Hao, X., Zhou, X., Liu, X., & Sang, X. (2016). Flow characteristics of external gear pumps considering trapped volume. *Advances in Mechanical Engineering*, 8(10). doi: 10.1177/1687814016674100

[38] Kaczmarczyk, T.Z., Żywica, G., & Ihnatowicz, E. (2016). Experimental investigation on a rotodynamic pump operating in the cogeneration system with a low-boiling working medium. *Transactions of the Institute of Fluid-Flow Machinery*, 134, 63–87.

[39] Njock, J.P., Ngangué, M.N., Sosso, O.T., & Nzengwa, R. (2023). Highlighting the effect of the lower operating limit of the condenser on ORC working fluids selection. *Results in Engineering*, 19, 101369. doi: 10.1016/j.rineng.2023.101369

[40] Ping, X., Yang, F., Zhang, H., Zhang, J., Xing, Ch., Yan, Y., Yang, A., & Wang, Y. (2023). Information theory-based dynamic feature capture and global multi-objective optimization approach for organic Rankine cycle (ORC) considering road environment. *Applied Energy*, 348, 121569. doi: 10.1016/j.apenergy.2023.121569

[41] Dhote, N., Khond, M., & Sankpal, R. (2023). Wear material determination and parameters optimization of an external gear pump by Taguchi technique. *Materials Today: Proceedings*, 72 (Part 3), 679–686. doi: 10.1016/j.matpr.2022.08.374

[42] Hernandez-Carrillo, I., Wood, Ch.J., & Liu, H. (2017). Advanced materials for the impeller in an ORC radial microturbine. *Energy Procedia*, 129, 1047–1054. doi: 10.1016/j.egypro.2017.09.241

[43] Li, W., & Yu, Z. (2021). Cavitating flows of organic fluid with thermodynamic effect in a diaphragm pump for organic Rankine cycle systems. *Energy*, 237, 121495. doi: 10.1016/j.energy.2021.121495

[44] Li, W., & Yu, Z. (2021). Cavitation models with thermodynamic effect for organic fluid cavitating flows in organic Rankine cycle systems. *Thermal Science and Engineering Progress*, 26, 101079. doi: 10.1016/j.tsep.2021.101079

[45] Li, W., Mckeown A., & Yu, Z. (2020). Correction of cavitation with thermodynamic effect for a diaphragm pump in organic Rankine cycle systems. *Energy Reports*, 6, 2956–2972. doi: 10.1016/j.egyr.2020.10.013

[46] Borsukiewicz-Gozdur A. (2013). Pumping work in the organic Rankine cycle. *Applied Thermal Engineering*, 51 (1–2), 781–786. doi: 10.1016/j.applthermaleng.2012.10.033

[47] Lu, Y., Guo, Z., Zheng, Z., Wang, W., Wang, H., Zhou, F., & Wang, X. (2023). Underwater propeller turbine blade redesign based on developed inverse design method for energy performance improvement and cavitation suppression. *Ocean Engineering*, 277, 114315. doi: 10.1016/j.oceaneng.2023.114315

[48] Bianchi, G., Fatigati, F., Murgia, S., & Cipollone, R. (2017). Design and analysis of a sliding vane pump for waste heat to power conversion systems using organic fluids. *Applied Thermal Engineering*, 124, 1038–1048. doi: 10.1016/j.applthermaleng.2017.06.083

[49] Kaczmarczyk, T.Z., Ihnatowicz, E., Żywica, G., & Kaniecki, M. (2019). Experimental study of the prototype of a Roto-Jet pump for the domestic ORC power plant. *Archives of Thermodynamics*, 40(3), 83–108. doi: 10.24425/ather.2019.129995

[50] Yang, Y., Zhang, H., Xu, Y., Yang, F., Wu, Y., & Lei, B. (2018). Matching and operating characteristics of working fluid pumps with organic Rankine cycle system. *Applied Thermal Engineering*, 142, 622–631. doi: 10.1016/j.applthermaleng.2018.07.039

[51] Yang, Y., Zhang, H., Tian, G., Yonghong, X., Chongyao, W., & Jianbing, G. (2019). Performance Analysis of a Multistage Centrifugal Pump Used in an Organic Rankine Cycle (ORC) System under Various Condensation Conditions. *Journal of Thermal Science*, 28, 621–634. doi: 10.1007/s11630-019-1069-9

[52] Zeleny, Z., Vodicka, V., Novotny, V., & Mascuch, J. (2017). Gear pump for low power output ORC – an efficiency analysis. *Energy Procedia*, 129, 1002–1009. doi: 10.1016/j.egypro.2017.09.227

[53] D'Amico, F., Pallis, P., Leontaritis, A.D, Karellas, S., Kakalis, N.M., Rech, S., & Lazzaretto, A. (2018). Semi-empirical model of a multi-diaphragm pump in an Organic Rankine Cycle (ORC) experimental unit. *Energy*, 143, 1056–1071. doi: 10.1016/j.energy.2017.10.127

[54] Carraro, G., Pallis, P., Leontaritis, A.D., Karellas, S., Vourliotis, P., Rech, S., & Lazzaretto, A. (2017). Experimental performance evaluation of a multi-diaphragm pump of a micro-ORC system. *Energy Procedia*, 129:1018-1025. doi: 10.1016/j.egypro.2017.09.232.

[55] Zardin, B., Natali, E., & Borghi, M. (2019). Evaluation of the Hydro-Mechanical Efficiency of External Gear Pumps. *Energies*, 12(13), 2468. doi: 10.3390/en12132468

[56] Misiewicz W. (2007). The optimization of the pump sets with the variable-speed drives. Maszyny Elektryczne – Zeszyty Problemowe, 78, 43–52.

[57] Yang, X., Xu, J., Miao, Z., Zou, J., & Yu, Ch. (2015). Operation of an organic Rankine cycle dependent on pumping flow rates and expander torques. *Energy*, 90(1), 864–878. doi: 10.1016/j.energy.2015.07.121

[58] Landelle, A., Tauveron, N., Revellin, R., Haberschill, P., Colasson, S., & Roussel, V. (2017). Performance investigation of reciprocating pump running with organic fluid for organic Rankine cycle. *Applied Thermal Engineering*, 113, 962–969. doi: 10.1016/j.applthermaleng.2016.11.096

[59] Feng, Y-Q., Hung, T-Ch., Wu, S-L., Lin, Ch-H., Li, B-X., Huang, K-Ch., & Qin, J. (2017). Operation characteristic of a R123-based organic Rankine cycle depending on working fluid mass flow rates and heat source temperatures. *Energy Conversion and Management*, 131, 55–68. doi: 10.1016/j.enconman.2016.11.004

[60] Yang, Y., Zhang, H., Xu, Y., Zhao, R., Hou, X., & Liu, Y. (2018). Experimental study and performance analysis of a hydraulic diaphragm metering pump used in organic Rankine cycle system. *Applied Thermal Engineering*, 132, 605–612. doi: 10.1016/j.applthermaleng.2018.01.001

[61] Gao, P., Wang, Z.X., Wang, L.W., & Lu, H.T. (2018). Technical feasibility of a gravity-type pumpless ORC system with one evaporator and two condensers. *Applied Thermal Engineering*, 145, 569–575. doi: 10.1016/j.applthermaleng.2018.09.049

[62] Komaki, K., Kanemoto, T., & Sagara, K. (2012). Performances and Rotating Flows of Rotary Jet Pump. *Open Journal of Fluid Dynamics*, 2(4A), 375–379. doi: 10.4236/ojfd.2012.24A048

[63] Osborn, S. (1996). The Roto-Jet pump: 25 years new. *World Pumps*, 363, 32–36. doi: 10.1016/S0262-1762(99)81000-1

[64] Jiang, L., Lu, H.T., Wang, L.W., Gao, P., Zhu, F.Q., Wang, R.Z., & Roskilly, A.P. (2017). Investigation on a small-scale pumpless Organic Rankine Cycle (ORC) system driven by the low temperature heat source. *Applied Energy*, 195, 478–486. doi: 10.1016/j.apenergy.2017.03.082

[65] Gkimisis, L., Arapkoules, N., Vasileiou, G., Soldatos, A., & Spitas, V. (2020). Modelling and numerical simulation of a novel Pumpless Rankine Cycle (PRC). *Applied Thermal Engineering*, 178, 115523. doi: 10.1016/j.applthermaleng.2020.115523

[66] Richardson, E.S. (2016). Thermodynamic performance of new thermofluidic feed pumps for Organic Rankine Cycle applications. *Applied Energy*, 161, 75–84. doi: 10.1016/j.apenergy.2015.10.004

[67] Semkło, Ł., & Gierz, Ł. (2022). Numerical and experimental analysis of a centrifugal pump with different rotor geometries. *Applied Computer Science*, 18(4), 82–95. doi: 10.35784/acs-2022-30

[68] Datla, B.V., & Brasz J.J. (2012). Organic Rankine Cycle System Analysis for Low GWP Working Fluids. *International Refrigeration and Air Conditioning Conference at Purdue*, 16–19 July, 2012

[69] Kaczmarczyk, T.Z., & Ihnatowicz, E. (2016). The experimental investigation of scroll expanders operating in the ORC system with HFE7100 as a working medium. *Applied Mechanics and Materials*, 831, 245–255

[70] Kaczmarczyk, T.Z., Żywica, G., & Ihnatowicz, E. (2017). The impact of changes in the geometry of a radial microturbine stage on the efficiency of the micro CHP plant based on ORC. *Energy*, 137, 530–543. doi: 10.1016/j.energy.2017.05.166

[71] Mathias, J.J., Johnston, J.J., Cao, J.J., Priedeman, D.D., & Christensen, R.N. (2009). Experimental testing of gerotor and scroll expanders used in, and energetic and exergetic modeling of an organic Rankine cycle. *Journal of Energy Resources Technology. Trans. ASME*, 131, 21–24. doi: 10.1115/1.3066345

[72] Kaczmarczyk, T.Z., Żywica, G., & Ihnatowicz, E. (2017). Measurements and vibration analysis of a five-stage axial-flow microturbine operating in an ORC cycle. *Diagnostyka*, 18(2), 51–58.

[73] Rausch, M.H., Kretschmer, L., Will, S., Leipertz, A., & Fröba, A.P. (2015). Density, Surface Tension, and Kinematic Viscosity of Hydrofluoroethers HFE-7000, HFE-7100, HFE-7200, HFE-7300, and HFE-7500. *Journal of Chemical Engineering*, 60, 3759–3765. doi: 10.1021/acs.jced.5b00691

[74] Bell, I.H., Wronski, J., Quoilin, S., & Lemort, V. (2014). Pure and Pseudo-pure Fluid Thermophysical Property Evaluation and the Open-Source Thermophysical Property Library CoolProp. *Industrial & Engineering Chemistry Research*, *53*(6), 2498–2508. doi: 10.1021/ie4033999

[75] Rządkowski, R., Żywica, G., Kaczmarczyk, T.Z., Koprowski, A., Dominiczak, K., Szczepanik, R., & Kowalski, M. (2020). Design and investigation of a partial admission radial 2.5-kW organic Rankine cycle micro-turbine. *International Journal of Energy Research*, 44(14), 11029–11043. doi: 10.1002/er.5670